2016 24th International Lightning Detection Conference &
6th International Lightning Meteorology Conference
18 - 21 April | San Diego, California, USA

Characteristics of a bipolar cloud-to-ground lightning flash containing a positive stroke followed by three negative strokes

Ye Tian, Xiushu Qie, Gaopeng Lu, Rubin Jiang, Zhichao Wang, Hongbo Zhang, Mingyuan Liu, Zhuling Sun
LAGEO, Key Laboratory of Middle Atmosphere and Global Environment Observation
Institute of Atmospheric Physics, Chinese Academy of Sciences
Beijing, China
qiex@mail.iap.ac.cn

Guili Feng
Atmospheric Observation center of Shandong Meteorological Bureau
Jinan, China

***Abstract*—Using time-correlated high-speed video images at 3,200 frames per second, broadband electric field change data and low-frequency magnetic fields, a natural bipolar cloud-to-ground (CG) lightning flash with one first positive stroke followed by three subsequent negative strokes is analyzed. All of these four strokes transferred electric charge to ground through the same lower channel with a time interval of 328 ms between the positive stroke and the first negative stroke. The flash onset was followed by several positive leaders that extended below the cloud base, one of which descended to culminate in a positive stroke with a continuing current. Another positive leader extended horizontally to a distant negative cloud region and induced several recoil leaders that intermittently retrograded along the leader channel. Eventually, three recoil leaders successively traversed along the path of positive stroke to produce respective negative strokes, resulting in the polarity reversal of charge transferred to ground. The average two-dimensional (2-D) speed of the positive leader was 1.1×10^5 m/s, while for 3 negative leaders was 6.7×10^6 m/s. The zero-crossing time and rise time of the radiation field waveform for the 3 negative strokes is smaller than the typical negative subsequent strokes, making them hard to be recognized as return strokes by the CG lightning location network.**

Keywords—bipolar cloud-to-ground flash; recoil leaders; charge sources; radar reflectivity

I. INTRODUCTION

The reversal in the polarity of charge transferred to ground has been observed for a small percentage (about 6%) of total cloud-to-ground (CG) lightning flashes [*Gorin and Shkilev*, 1984]. As for upward lightning, this ratio could be much higher (roughly 20%) for winter thunderstorms in Japan [*Goto and Narita*, 1995]. In these flashes, usually termed as bipolar flashes, both positive and negative charges are lowered to ground, through the identical lower part of a lightning channel near the ground.

The reported observations of bipolar flashes are mostly associated with upward lightning that usually starts with an upward leader from the top of elevated objects [e.g., *Hubert et al.*, 1984; *Wang and Takagi*, 2008; *Zhou et al.*, 2011], and the cases involving an initial downward leader are relatively infrequent. *Jerauld et al*. [2009] reported a natural downward bipolar flash containing two stroke locations with electric and magnetic field measurements. *Fleenor et al*. [2009] presented four bipolar flashes occurring in the Central Great Plains by using video recording system records and the National Lightning Detection Network (NLDN) Database. *Nag and Rakov* [2012] examined two bipolar flashes only with electric field data, whereas there were no available GPS time and NLDN records for the first bipolar flash and the positive stroke of the second bipolar flash may be an intra-cloud discharge based on the NLDN report. Recently, *Chen et al*. [2015] documented a downward bipolar lightning flash that contained one first positive stroke with a peak current of 142 kA and five subsequent negative strokes hitting on a 90 m tall structure. *Xue et al.* [2015] obtained the spectra of a natural bipolar cloud-to-ground lightning.

It is commonly observed that the bipolar flashes with an initial downward leader occur as a combination of positive CG and negative CG flashes with their respective features. That is,

these bipolar CG flashes often contain a first stroke of positive polarity with a continuing current, as well as several subsequent negative strokes; the interval between the positive stroke and the first negative stroke is often longer than 100 ms [e.g., *Saba et al.*, 2013]. The reversal in the polarity of strokes reflects the change in the polarity of descending leaders prior to the return stroke. *Saba et al.* [2013] attributed the negative leader preceding the negative stroke to the recoil leader that retrogrades along the path of the positive leader during the early development of flashes. The analyses of *Saraiva et al.* [2014] based on the three-dimensional (3-D) lightning mapping observation of a bipolar flash confirmed this scenario; in addition, *Saraiva et al.* [2014] also reported one case of bipolar flash where the recoil leader might branch to create a new lightning path to reach the ground, leading to bipolar flashes with multiple channels.

The bipolar flashes in which the strokes deposit electric charge of opposite polarities to ground through the identical channel are very rare, and more observations are desired to formulate a general formation mechanism of polarity reversal in CG lightning strokes. In this paper, we report the analyses of a natural bipolar lightning flash observed by a high-speed camera during the summer campaign in 2014 at the SHandong Artificially Triggering Lightning Experiment (SHATLE) [*Qie et al.*, 2011]. This flash contained one positive stroke followed by three negative strokes that all deposited charge to ground through the same channel below the cloud. Comprehensive measurements, including broadband electric field (E-field) change, magnetic field, surface electrostatic field, and radar reflectivity, are used to investigate the physical process of this bipolar CG flash and examine the waveform characteristics of negative strokes which have rarely been reported previously.

II. Observations and Measurements

The bipolar CG flash reported here was captured at 12:31 UTC (Beijing time 20:31) on July 14, 2014. This flash was observed from the main observation site (37.8284 °N, 118.1150 °E) of SHATEL at a frame rate of 3,200 frames per second (fps) with a Phantom M310 video camera equipped with a F1.4 Nikon lens with a focal length of 28 mm; the image resolution is 1280 × 800 pixels. The concurrent measurements were obtained at the same location through a slow E-field change antenna, a fast E-field change antenna [*Jiang et al.*, 2013; *Qie et al.*, 2014], and a low-frequency (LF) magnetic sensor (two perpendicular loop antennas) [*Lu et al.*, 2013, 2014]. The parameters of instruments that contribute to the analysis of this flash are listed in Table 1. All the measurements were synchronized through a GPS receiver with timing accuracy better than 100 ns, which makes it possible to compare the visual development of the flash with recorded electromagnetic signals. The physical sign convention is adopted for the polarity of electric field, i.e., positive E corresponds to negative charge overhead. With this definition, a negative CG stroke that lowers negative charge to ground will induce negative surface E-field change; for an assumed cylindrical coordinate system with the negative CG stroke located at the origin, a positive azimuthal magnetic field is measured at the location of magnetic sensor, namely counterclockwise.

TABLE 1. PARAMETERS OF INSTRUMENTS THAT ACQUIRED DATA FOR THE ANALYSIS.

Instrument	3-dB bandwidth	Sampling rate	Time constant
Slow E-field change antenna	~10 Hz-1 MHz	5 MHz	0.22 s
Fast E-field change antenna	1 kHz-2 MHz	5 MHz	0.1 ms
Low-frequency magnetic field	3-300 kHz	1 MHz	N.A.

Radar reflectivity data were obtained from a meteorological radar located in Jinan (36.80 °N, 116.78 °E, 160 km from the stroke), Shandong Province. The weather balloon sounding data from Zhangqiu station (36.70 °N, 117.55 °E), about 135 km from the stroke location, at 12:00 UTC on July 14, 2014 were used to infer the environmental temperature profile of the thunderstorm.

III. Analysis Of Flash Development

A. *General Characteristics and Waveform Parameters of the Strokes*

The multi-disciplinary measurements for the bipolar flash are shown in Figure 1. The slow (black curve) and fast E-field change data (blue curve) consistently indicate that this flash contained one positive stroke and three subsequent negative strokes (as indicated in the figure) over an overall duration of about 817 ms. The pre-stroke in-cloud activity lasted about 120 ms after the flash onset that was visible on all the measurements, which is typical for first positive strokes [*Rust et al.*, 1981; *Fuquay*, 1982; *Kong et al*, 2008; 2015]. As indicated by the luminosity data (red curve) based on high-speed images, the positive stroke was followed by a long continuing current of ~80 ms; the small variations superposed on the sustained brightening of lighting channel indicate the occurrence of *M*-processes, as suggested by the corresponding small deflections in electric and magnetic fields. During a subsequent time interval of ~220 ms prior to the first negative stroke, seven *K*-processes occurred with clear electric and magnetic variations. The 328 ms interval between the positive stroke and the first negative stroke was relatively long in comparison with other observations of bipolar flashes; the inter-stroke interval between three negative CG strokes was 104.4 ms and 111.2 ms, respectively. The third (last) negative stroke was also followed by a relatively short continuing current of about 20 ms.

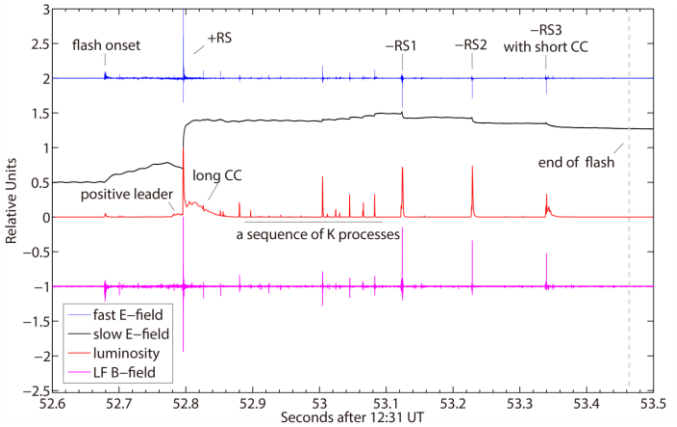

Fig. 1. Comprehensive measurements for the bipolar cloud-to-ground flash. For the convenience of comparison, all the data are normalized by the maximum value (and shifted vertically).

The positive stroke was located by the Lightning Location System (LLS) of the State Grid Corporation of China. The LLS covers most parts of China and locates CG lightning using a similar principle as the U.S. NLDN. The location error of the LLS for CG lightning is <1000 m in our observation area of Shandong Province [*Chen et al.*, 2008]. We compared the location result by LLS with the position of a rocket-triggered lightning in SHATLE and found the location error is less than 800 m. The LLS-reported peak current of the positive return stroke for this bipolar flash is 68.4 kA, and is located about 14.3 km northwest of the observation site. This location appears to be reasonable as the E-field variation before the positive stroke and suggests that this stroke occurred far from the so-called "reversal distance" (roughly 7-9 km) regarding the polarity of electric field change caused by a descending lightning leader prior to the return stroke [*Beasley et al.*, 1982].

It is interesting to note that the following 3 negative return strokes were not located by the LLS, and they were misclassified as intra-cloud lightning flashes, similar to the case analyzed by *Nag and Rakov* [2012]. In order to conjecture the cause of the misclassification, we analyzed the parameters of microsecond-scale electric field waveforms produced by the three negative return strokes and compared them with previously reported characteristic values of both positive and negative return strokes, as shown in Table 2. It can be seen that the initial electric field peak normalized to 100 km (geometric mean) of three negative return strokes was close to the value (geometric mean) of those subsequent negative return strokes reported in Florida, but was 4.6 times smaller than the counterpart (arithmetic mean) for positive return strokes and 3.3 times smaller than that for the positive stroke in the same flash. Note that the arithmetic mean zero-crossing time of three negative strokes in this bipolar flash was almost 8 times smaller than the statistical result of negative subsequent return strokes, which may be the partial reason for misclassification of these negative strokes by the LLS. Shorter zero-to-peak rise time and 10%-90% peak rise time of the three negative return strokes indicated that they could produce stronger radiation electromagnetic field than normal negative strokes with similar electric field peak. In addition, the rest parameters of three negative strokes, listed in Table 2, were much smaller than those of referenced negative and positive return strokes. It should be noted that because the zero-to-peak rise time of the second negative return stroke was only 0.4 μs, the last three parameters for this return stroke could not be determined through the fast E-field waveform. Compared with normal negative strokes, the shorter and smaller characteristics of negative strokes in the bipolar CG flash indicated charges with opposite polarity flowed along the same channel, in the order of firstly positive and then negative, would own different physical processes, such as the change of channel conductivity and residual positive charge's effect on the following negative charge.

TABLE 2. PARAMETERS OF ELECTRIC FIELD WAVEFORMS FROM FAST ANTENNA.

Parameter	+RS	1th -RS	2nd -RS	3rd -RS	AM	Reference value of +RS	Reference value of subsequent -RS
Initial peak (V/m) (normalized to 100 km)	10.0	3.8	3.0	2.4	3.0 (GM)	13.9	2.7 (GM)
Zero-crossing time (μs)	41.5	5.3	3.7	5.6	4.9	151	39
Zero-to-peak rise time (μs)	17.3	1.6	0.4	2.0	1.3	6.9	2.8
10-90 percent rise time (μs)	4.3	1.1	0.3	0.7	0.7	6.2	1.5
Slow front duration (μs)	16.9	1.3	≤0.2	1.6	1.5	10	2.1
Slow front, amplitude as percentage of peak	53	25.3	N.A.	12.3	18.8	64	40
Fast transition, 10-90 percent rise time (ns)	300	310	N.A.	320	315	560	610

Note: Reference values of both positive and negative RS are arithmetic mean values adapted from Rakov and Uman (2003). AM and GM represents arithmetic mean value and geometric mean value of three negative strokes, respectively.

In order to better understand the return stroke processes, we show the fast electric field waveforms over 100 μs interval for all the four return strokes in Figure 2. It can be seen from the Figure that all three negative return stroke exhibited similar characteristics that are different from normal subsequent negative return strokes [*Nag et al.*, 2008, Figure 1 c and d]. First of all, some fluctuations existed in the initial part of rising edge of return strokes; secondly, return strokes at distance of 14.3 km were followed by opposite-polarity overshoots, which were 13.5%, 18.8%, 7.5% of the peak for the three negative return stroke, respectively. According to *Haddad et al.* (2012), the percentage of subsequent negative strokes exhibiting an opposite polarity overshoot, within the distance of 50 km, is only 11%; and thirdly, fluctuations were superimposed on the falling edge of return strokes as well. These characteristics may likely be caused by the complicated intra-cloud discharges accompanying the negative strokes.

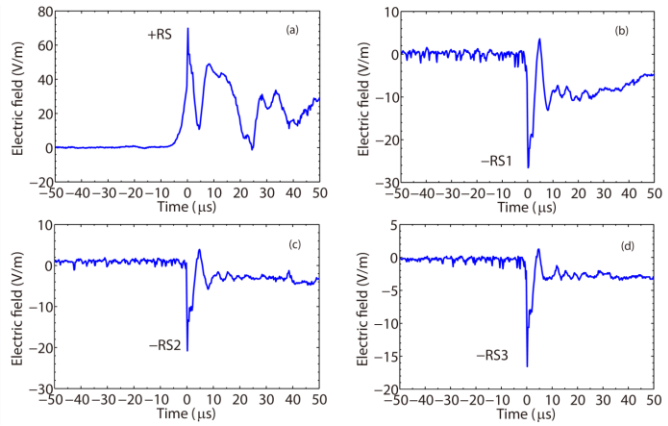

Fig. 2. Fast electric field change waveform over 100 μs in the bipolar flash: (a) first positive return stroke; (b) subsequent negative return stroke; (c) second negative return stroke; (d) third negative return stroke. In each panel, the time is given relative to the peak of the electric field change waveform.

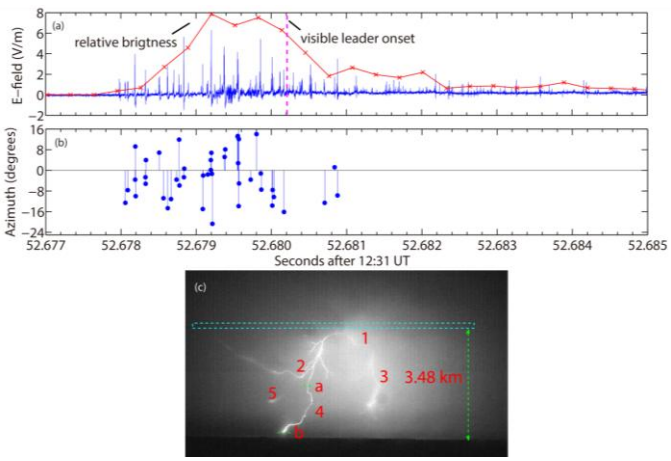

Fig. 3. (a) Fast electric field and relative brightness of preliminary breakdown pulse train with same time coordination of (b) (Purple line indicates the time when positive leader become visible); (b) azimuth of measured magnetic field of preliminary breakdown pulse train (Azimuth is relative to the visible point of the initial descending positive leader); (c) a superposition of selected frames of the high-speed video for the development of downward positive leader. Number order represents the sequence of several leaders.

B. Flash Initiation and Initial Leader Development

Figure 3a shows the fast electric field and relative brightness captured by the high-speed camera of preliminary breakdown process for the bipolar CG flash. Based on the electric field record, flash inception occurred at 52.678 s. A visible light burst was detected almost immediately after flash initiation, within 0.5 ms. The initial descending leader was not seen until 2.2 ms after flash initiation, as indicated by the purple line in Figure 3a. These observational facts strongly suggest that the flash onset was very close to the bottom of the thunderclouds (at about 3.48 km above sea level). The light burst lasted about 3 ms, during which both electric and magnetic signals exhibit the characteristic train of preliminary breakdown pulses (PBPs). As shown in Figure 3a, the initial polarity of these pulses is the same as the following positive return stroke. During the major duration of PBPs, the typical inter-pulse interval was between 30 and 50 μs. The ratio between the signals in two-perpendicular antennas of the magnetic sensor can be used to calculate the azimuth of the radiation pulses source. The azimuth relative to the visible point of the initial descending positive leader is shown in Figure 3b. The variation in azimuth implies the possible region for the sources of preliminary breakdown pulses, as indicated in Figure 3b and cyan lines in Figure 3c. The upper and lower cyan lines, namely the width of the box, are corresponding to the largest possible propagation distance, estimated by multiplying the initial propagating speed of the positive leader and time difference between initial signals of preliminary breakdown and the visible point of the initial descending positive leader. It should be noted that the computational region is much larger than the general positive leader origin [e.g., *Lu et al.*, 2009], indicating that the horizontal discharges might produce detectable magnetic field as well and should not be neglected as it is done usually.

During the 118 ms interval from the flash initiation to the positive stroke, the high-speed camera recorded the propagation of several positive leaders. Based on the bi-directional propagation theory, it implies that there might be a distribution of negative charge deposited near the cloud base. The paths of several major positive leaders whose propagation can be readily discerned in high-speed images are marked in Figure 3c, where the number indicates the sequence of leader development ordered by time; other branches visible in the figure are mainly manifested through recoil leaders. The average 2-dimensional (2D) speed of the positive leader (along path 4) propagating from point *a* to point *b* in Figure 3c is estimated to be 1.1×10^5 m/s with a clear trend of accelerating from 5.9×10^4 m/s to 1.5×10^5 m/s while the leader approached the ground, in comparison with 5.44×10^4 m/s, 1.15×10^5 m/s and 8.96×10^4 m/s for other positive leaders respectively along paths 1, 2, and 5 in Figure 3c that did not reach the ground. Of course, the observed difference in leader speed could be due to the effect of 2-D velocity measurement instead of 3-D.

C. First Positive Stroke

The first stroke with positive polarity occurred about 120 ms after the flash onset. As shown in Figure 4a, the leader propagation between point *a* and ground surface shown in Figure 3c is responsible for the enhancement of channel brightness beginning at 52.78 s. However, the descending leader prior to the return stroke did not cause discernible variations in the fast electric and magnetic field. Electromagnetic signals sometimes linked to stepping features in positive leaders have been reported in the literature using measurements within 1 km of the leader channel [e.g., *Biagi et al.*, 2011; *Lu et al.*, 2014]. No discernible electric and magnetic field variations during the leader stage indicate that the positive leader for this flash was not stepped.

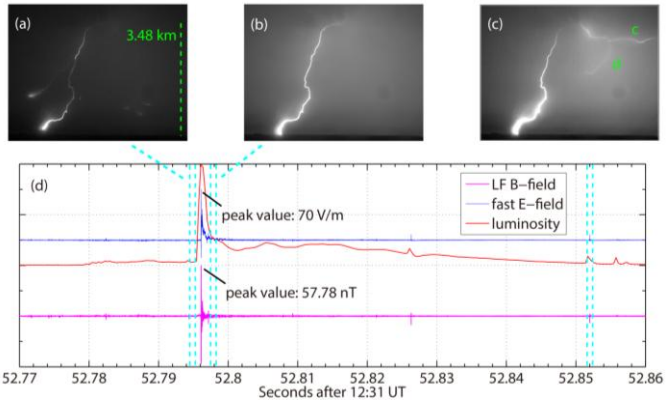

Fig. 4. (a) The high-speed video image of the positive leader at 52.795852 s; (b) the high-speed video image of the continuing current at 52.798977 s; (c) the superposed high-speed video image of five frames of recoil leaders from 52.85179 s to 52.85304 s, c and d are two paths of recoil leaders; (d) characteristics of broadband electromagnetic radiations associated with the positive stroke in the bipolar flash.

The persistent brightness of lightning channel after return stroke indicates that the positive return stroke was followed by a long continuing current of about 80 ms. There were several recoil leaders apparently merging into the stroke channel during the continuing current; Figure 4c shows two such recoil leaders that propagated by traversing lightning paths explored by the previous positive leaders. The lightning path d that appears to extend away from the observation site will be traversed by more recoil leaders during the remaining period of the flash, and this lightning path acted as the main conduit for the transportation of negative charge from a distant negative cloud charge region to ground through the channel of the positive stroke.

D. Subsequent Negative Strokes

When the channel became dim after the positive stroke, a sequence of *M*-components occurred and caused discernible electromagnetic deflections. The *K*-processes following the *M*-components, occurred near the base of the cloud, lit up the lightning channels explored by positive leaders that did not terminate on the ground. In particular, the *M*-components before 53.0 s (relatively weak) were results of recoil leaders connecting with the main channel, in which former four recoil leaders propagated along path c and latter four recoil leaders propagated along path d in Figure 4c, and the seventh recoil leader recoiled twice in succession; all the *K*-processes after 53.0 s propagated along the same path in Figure 5b, and they were typically brighter than earlier *M*-components. The bright and intermittent recoil leaders occurring after 53.0 s, some of which were also attempted dart leaders, may have played a critical role in maintaining the conductivity of the lightning channels and formed the negative leader finally leading to the negative strokes ultimately. Indeed, as shown in Figure 5b, the negative leader preceding the first negative stroke incipiently propagated along the same path of recoiling leaders recurring after 53.0 s and then followed the channel of positive stroke to reach the ground. This negative leader was associated with a burst of microsecond-scale electromagnetic pulses for about 2.2 ms (and the associated light burst), indicating that there were step-like characteristics in the propagation of the negative leader on account of the time interval of about 40 ms between the last *K*-process and the first negative leader which might lead to a slightly lower conductivity of the channel (refer to Figure 5b). We inspected the magnetic field data measured by our sensitive magnetic field sensor for other negative return strokes located by the LLS from 12:00 to 13:00 UTC and found almost all return strokes were not preceded by a burst of microsecond-scale pulses, which implies that the burst of pulses might cause that three negative strokes of this bipolar flash were misclassified as intra-cloud lightning by the LLS. The average 2-D speed of the descending negative leader is estimated to be 4.32×10^6 m/s, similar to the typical value for dart negative leaders [*Saraiva et al.*, 2014]. In the macroscopic view, channels of all negative leaders were clear and convergent, without branching.

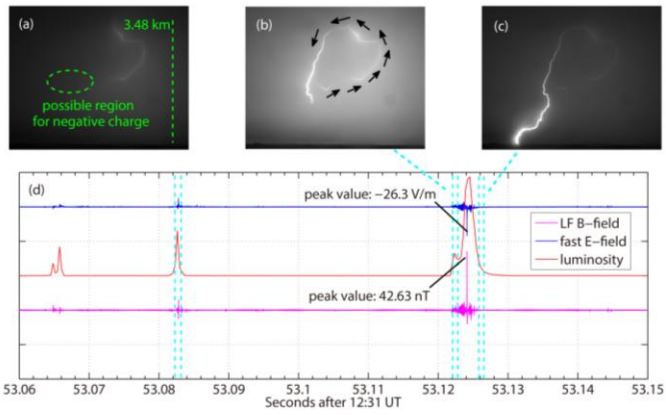

Fig. 5. (a) The high-speed video image of the last *K*-process at 53.082727 s; (b) the superposed high-speed video image of two frames of the first negative leader at 53.122727 s to 53.123665 s; (c) the high-speed video image of the first negative return stroke at 53.126165 s; (d) characteristics of broadband electromagnetic radiations associated with the first negative stroke in the bipolar flash.

The remaining two negative strokes in the flash occurred with the preceding leader appearing to originate from the same cloud region as the first negative stroke. Both return strokes were preceded by dart leaders (with duration of 0.9 ms and 1.9 ms, respectively), and the average 2-D speed of negative leader prior to these two strokes is estimated to be 8.74×106 m/s and 7.05×106 m/s, respectively.

IV. Meteorological Background of the Bipolar Cloud-to-Ground Flash

At 11:02 UTC, a supercell thunderstorm began to move toward the observation site as shown in Figure 6a. When the thunderstorm developed to its mature stage, it tended to split into three parts at 11:32 UTC (referring to Figure 6b), and evolved into the 3 cells as shown in Figure 6c. At 12:03 UTC, the small cell 2 had separated from the main cell 1 and was 14.7 km from the observation site. During the bipolar flash, the small cell, with an area of around 83 km^2, developed to its dissipating stage, and its front edge began to pass over the main observation site. As shown in Figure 6d, this flash was rooted in the small convective cell separated from the main body of the parent thunderstorm which was moving eastward to the north of the observation site. Half an hour after the bipolar flash, the small cell disappeared but the main cell

remained in the same place as it was at 12:33 UTC. The average velocity of the parent thunderstorm between 11:30 UTC and 13:00 UTC was about 18 km/h. The cross section of radar reflectivity along the black and dashed line across the observation site in Figure 6d shows that the height of cloud top was about 9 km (Figure 6f), which indicates the intensity of the small cell was weaker. Based on the closest weather balloon sounding at 12:00 (UTC) at Zhangqiu, the height rose from approximately 4 km to 7.4 km when the environmental temperature declined from 0 ℃ to -20 ℃ which is the range where negative charge usually lives [Coleman et al., 2006]. Although the temperature profiles at distances far from the storm may not always well correlate with the location of the charge layers inside the thunderstorm, it can be used for supplement to refer the environmental temperature profiles around the storm. This inferred height region from 4 km to 7.4 km corresponding to a possible electrification region inside the cloud is in agreement with the radar echo, supporting that this could be a reasonable charge region. A total of 7 CG flashes were located by the LLS in the 10 minutes before and after the bipolar flash, among them 5 were positive CG flashes, and 2 were negative CG flashes. Arrows in Figure 7 represent the occurrence of partial positive CG flashes in the cyan rectangle of Figure 6d.

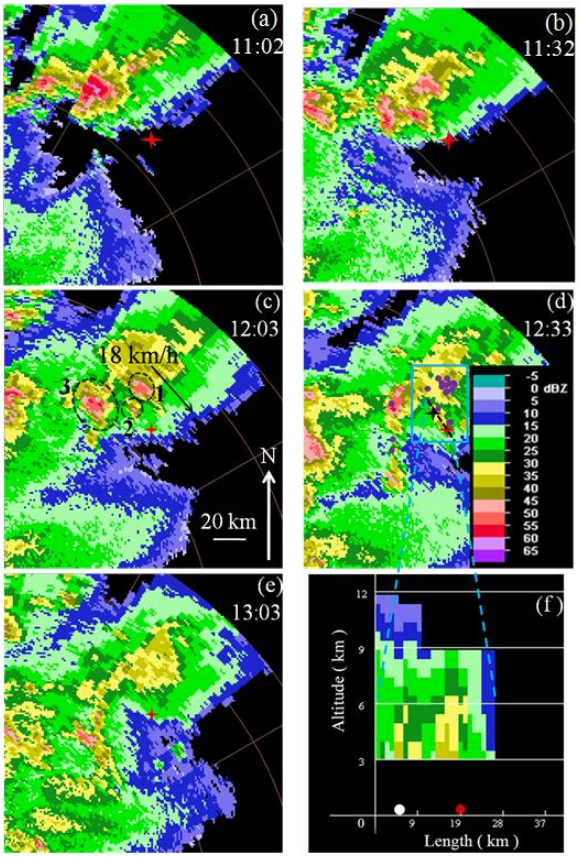

Figure 6. Composite reflectivity of the thundercloud at (a) 11:02 UTC ; (b) 11:32 UTC ; (c) 12:03 UTC ; (d) 12:33 UTC; (e) 13:03 UTC. (f) Cross-section of the composite reflectivity at 12:33 UTC along the black dashed line in (d) which also points the direction that the camera is facing. Black and red star show the location of the strokes and the main observation site respectively which are also marked as white and red circles in (f), and purple circles represent positive CG strokes located by the lightning location system from 12:00 UTC to 13:00 UTC in (d). Moving direction and average speed of the thunderstorm is indicated in (c). Distance is shown by the white line segment in (c).

The surface electric field measured by an electric field mill located at the main observation site, as shown in Figure 7, indicates a significant negative change from positive began at about 12:00 UTC and continued until 12:40 UTC.

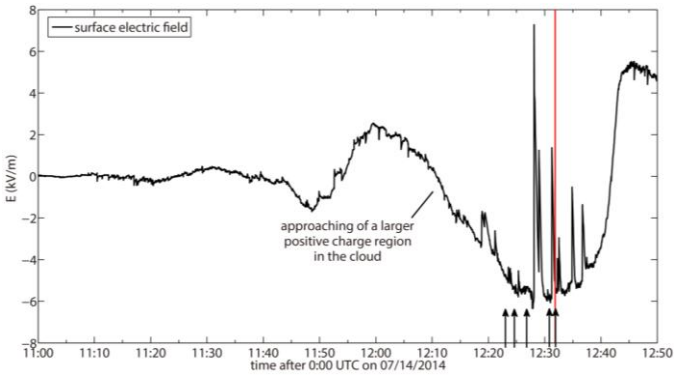

Fig. 7. Evolution of surface electrostatic field during the thunderstorm. Red line shows the time of occurrence for the bipolar flash. Positive CG flashes occurred in the cyan rectangle of Figure 6d are marked by arrows.

As most of the graupels fell to the ground in the dissipating stage of the storm, the lower main negative charge in the thunderstorm decreased, and the positive CG flashes from the upper positive region might overwhelmingly dominate [*Qie et al.*, 2005; *Zhang et al.*, 2015]. Besides, because of the wind shear, the positive stroke in the bipolar CG flash might initiate from the anvil in the front of the cloud along the moving direction of the small storm cell. Therefore, the partial positive charge in the anvil might be exposed to the ground. Some descending positive charge in the anvil interacted with a few underneath remaining negative charge to create initial paths for the following charge transportation.

V. CONCLUSIONS

A natural bipolar cloud-to-ground lightning flash with one first positive stroke followed by three subsequent negative strokes was analyzed in detail based on the high-speed video images acquired at 3,200 frames per second together with simultaneous broadband E-field change, low-frequency magnetic fields, surface electrostatic field and the weather radar echoes. The preliminary breakdown occurred in the cloud anvil region in the dissipating stage, leading to the formation of multiple positive leaders that descended from the bottom of storm cell and extended in several directions. One of them propagated downward to reach the ground, leading to the positive stroke; meanwhile, other positive leaders progressed horizontally to a laterally displaced negative charge region, and recoil leaders occurred intermittently to maintain the connection with the main stroke channel. Some of the recurring recoil leaders evolved into dart leaders down the channel to the ground, eventually resulting in a negative stroke, completing the polarity reversal of charge transfer to ground, and more leader-stroke sequences might occur as that happens in ordinary multi-stroke negative CG flashes. This scenario is generally the same as described by *Saba et al.* [2013] and

Saraiva et al. [2014]. The recoil leaders after the positive return stroke played a critical role in maintaining a connection between the channel to ground and the leader network in the cloud. This allowed the formation of the negative dart leaders which eventually culminated in negative CG return strokes. Based on the high speed video images, the average 2-D speed of the positive leader is 1.1×10^5 m/s, while for 3 negative leaders is 6.7×10^6 m/s.

Although the progression of positive and negative leaders, together with the corresponding waveform parameters of the return strokes in the bipolar CG flash is analyzed, the inception of the bipolar CG flash inside the cloud still keeps unopened. It will be interesting and important to further analyze the 3D bipolar lightning progression inside the cloud and to infer the lightning-related charge structure using the VHF mapping system. Observations and studies on the bipolar flash using VHF mapping system together with the measurements used in this paper will be continued in the future.

ACKNOWLEDGMENT

This work is supported jointly by National Key Basic Research and Development Program (973) "Dynamic-microphysical-electrical processes in severe thunderstorms and lightning hazards" (Grant No 2014CB441405), "The Hundred Talents Program" of Chinese Academy of Sciences (Grant No 2013068) and National Natural Science Foundation of China (Grant Nos 41405008, 41375012).

REFERENCES

Biagi, C. J., M. A. Uman, J. D. Hill, and D. M. Jordan (2011), Observations of the initial, upward-propagating, positive leader steps in a rocket-and-wire triggered lightning discharge, Geophys. Res. Lett., 38, L24809, doi: 10.1029/2011GL049944.

Beasley, W., M. A. Uman, and P. L. Rustan Jr. (1982), Electric fields preceding cloud-to-ground lightning flashes, J. Geophys. Res., 87, 4883-4902.

Campos, L.Z.S., and M.M.F.Saba (2013), Visible channel development during the initial breakdown of a natural negative cloud-to-ground flash, Geophys. Res. Lett., 40,doi:10.1002/grl.50904.

Chen, L., W. Lu, Y. Zhang, and D. Wang (2015), Optical progression characteristics of an interesting natural downward bipolar lightning flash, J. Geophys. Res. Atmos., 120, doi:10.1002/2014JD022463.

Chen, J.H., Zhang Q., Feng W. X., Fang Y. H. (2008), Lightning Location System and Lightning Detection Network of China Power Grid, High Voltage Engineering (In Chinese), 34(3), 425-431.

Coleman, L. M., T. C. Marshall, M. Stolzenburg, T. Hamlin, P. R. Krehbiel, W. Rison, and R. J. Thomas (2003), Effects of charge and electrostatic potential on lightning propagation, J. Geophys. Res., 108(D9), 4298, doi:10.1029/2002JD002718.

Fleenor, S. A., C. J. Biagi, K. L. Cummins, E. P. Krider, and X. M. Shao (2009), Characteristics of cloud-to-ground lightning in warm-season thunderstorms in the Central Great Plains, Atmos. Res., 91, 333–352, doi:10.1016/j.atmosres.2008.08.011.

Fuquay, D. M. (1982), Positive cloud-to-ground lightning in summer thunderstorms, J. Geophys. Res., 87,7131–7140, doi:10.1029/JC087iC09p07131.

Gorin B. N., and A V. Shkilev (1984), Measurement of lightning currents at the Ostankino tower, Electrichestvo, 8: 64-65.

Goto Y., and K. Narita (1995), Electric characteristics of winter lightning, J Atmos Ter Phys, 57 (5) : 449-508.

Haddad, M. A., V. A. Rakov, and S. A. Cummer (2012), New measurements of lightning electric fields in Florida: Waveform characteristics, interaction with the ionosphere, and peak current estimates, J. Geophys. Res., 117, D10101, doi:10.1029/2011JD017196.

Hubert P., P. Laroche, A. Eybert-Berard, and L. Barret (1984), Triggered lightning in new Mexico, J. Gephys. Res., 89 (D2) : 2511-2521.

Idone V P, Oville R E, Mach D M. (1987), The propagation speed of a positive lightning current return stroke, Geophys. Res. Lett., 14(11) : 1150-1153.

Jerauld, J. E., M. A. Uman, V. A. Rakov, K. J. Rambo, D. M. Jordan, and G. H. Schnetzer (2009), Measured electric and magnetic fields from an unusual cloud-to-ground lightning flash containing two positive strokes followed by four negative strokes, J. Geophys. Res., 114, D19115, doi:10.1029/2008JD011660.

Jiang, R., X. Qie, C. Wang, J. Yang (2013), Propagating features of upward positive leaders in the initial stage of rocket-triggered lightning, Atmos. Res., 129–130: 90–96, http://dx.doi.org/10.1016/j.atmosres.2012.09.005.

Kong X., X. Qie, Y. Zhao (2008), Characteristics of downward leader in a positive cloud-to-ground lightning flash observed by high-speed video camera and electric field changes, Geophys. Res. Lett., 35, L05816, doi:10.1029/2007GL032764.

Kong, X. Y. Zhao, T. Zhang, H. Wang (2015), Optical and electrical characteristics of in-cloud discharge activity and downward leaders in positive cloud-to-ground lightning flashes, Atmos. Res., 160, 28-38.

Lu, G., S. A. Cummer, J. Li, F. Han, R. J. Blakeslee, and H. J. Christian (2009), Charge transfer and in-cloud structure of large-charge-moment positive lightning strokes in a mesoscale convective system, Geophys. Res. Lett., 36, L15805, doi:10.1029/2009GL038880.

Lu, G., *et al.* (2013), Coordinated observations of sprites and in-cloud lightning flash structure, J. Geophys. Res., 118, 6607–6632, doi:10.1002/jgrd.50459.

Lu, G., R. Jiang, X. Qie, H. Zhang, Z. Sun, M. Liu, Z. Wang, and K. Liu (2014), Burst of intracloud current pulses during the initial continuous current in a rocket-triggered lightning flash, Geophys. Res. Lett., 41, 9174–9181, doi:10.1002/2014GL062127.

Nag, A., and V. A. Rakov (2012), Positive lightning: An overview, new observations, and inferences, J. Geophys. Res.,117, D08109, doi:10.1029/2012JD017545.

Nag, A., V. A. Rakov, W. Schulz, M. M. F. Saba, R. Thottappillil, C. J. Biagi, A. Oliveira Filho, A. Kafri, N. Theethayi, and T. Gotschl (2008), First versus subsequent return-stroke current and field peaks in negative cloud-to-ground lightning discharges, J. Geophys. Res., 113, D19112, doi:10.1029/2007JD009729.

Qie X., Kong X., Zhang G., et al. (2005), The possible charge structure of thunderstorm and lightning discharges in northeastern verge of Qinghai-Tibetan Plateau, Atmos. Res., 76(1-4): 231-246.

Qie, X., R. Jiang, C. Wang, J. Yang, J. Wang, *and* D. Liu (2011), Simultaneously measured current, luminosity, and electric field pulses in a rocket-triggered lightning flash, J. Geophys. Res., 116, D10102, doi:10.1029/2010JD015331.

Qie, X. S., R. B. Jiang, J. Yang (2014). Characteristics of current pulses in rocket-triggered lightning, Atmos. Res., 135–136, 322–329, http://dx.doi.org/10.1016/j.atmosres.2012.11.012.

Rakov, V. A., M. A. Uman, G. R. Hoffman, M. W. Masters, and M. Brook (1996), Bursts of pulses in lightning electromagnetic radiation: Observations and implications for lightning test standards, IEEE Trans. Electromagn. Compat., 38(2), 156–164, doi:10.1109/15.494618.

Rakov, V.A., and M.A. Uman (2003), Lightning: Physics and Effects, Cambridge Univ. Press, New York.

Rust, W. D., D. R. MacGorman, and R. T. Arnold (1981), Positive cloud-to-ground lightning flashes in severe storms, Geophys. Res. Lett., 8, 791–794, doi:10.1029/GL008i007p00791.

Saba, M.F., C. S chumann, T. A. Warner, J. H. Helsdon Jr., W. Schulz, and R. E. Orville (2013), Bipolar cloud-to-ground lightning flash observations, J. Geophys. Res., 118, 11,098–11,106, doi:10.1002/jgrd.50804.

Saba, M.F., K. L. Cummins, T.A.Warner, E. P. Krider, L. Z. S. Campos, M. G. Ballarotti, O. Pinto Jr., and S. A. Fleenor (2008), Positive leader characteristics from high-speed video observations, Geophys. Res. Lett., 35, L07802, doi:10.1029/2007GL033000.

Saraiva, A. C. V., et al. (2014), High-speed video and electromagnetic analysis of two natural bipolar cloud-to-ground lightning flashes, J. Geophys. Res. Atmos., 119, 6105–6127, doi:10.1002/2013JD020974.

Xue, S., P. Yuan, J. Cen, Y. Li, and X. Wang (2015), Spectral observations of a natural bipolar cloud-to-ground lightning, J. Geophys. Res. Atmos., 120, 1972–1979, doi:10.1002/2014JD022598.

Yoshida, S., et al. (2012), The initial stage processes of rocket-and-wire triggered lightning as observed by VHF interferometry, J. Geophys. Res., 117, D09119, doi:10.1029/2012JD017657.

Zhang, T., Z. Zhao, Y. Zhao, C. Wei, H. Yu, F. Zhou (2015), Electrical soundings in the decay stage of a thunderstorm in the Pingliang region, Atmos. Res., 164:188-193.

Zhou, H., G. Diendorfer, R. Thottappillil, H. Pichler, and M. Mair (2011), Characteristics of upward bipolar lightning flashes observed at the Gaisberg Tower, J. Geophys. Res., 116, D13106, doi:10.1029/2011JD015634.